Lavado-Garcia, J., Jorge, I., Cervera, L., Vazquez, J., & Godia, F. (2020). Multiplexed Quantitative Proteomic Analysis of HEK293 Provides Insights into Molecular Changes Associated with the Cell Density Effect, Transient Transfection, and Virus-Like Particle Production. *Journal of Proteome Research, 19*(3), 1085-1099. doi:10.1021/acs.jproteome.9b00601

Multiplexed quantitative proteomic analysis of HEK293 provides insights of molecular changes associated to the cell density effect, transient transfection and virus-like particles production.

Authors: Jesús Lavado-García*[1], Inmaculada Jorge[2-3], Laura Cervera[1], Jesús Vázquez[2-3], Francesc Gòdia[1]

[1]Grup d'Enginyeria Cellular i Bioprocés, Departament d'Enginyeria Química, Biològica i Ambiental, Escola d'Enginyeria, Universitat Autònoma de Barcelona, Campus de Bellaterra, Cerdanyola del Vallès, 08193 Barcelona, Spain

[2]Laboratory of Cardiovascular Proteomics, Centro Nacional Investigaciones Cardiovasculares (CNIC), C/ Melchor Fernández Almagro 3, Madrid 28029, Spain

[3]Centro de Investigación Biomédica en Red Enfermedades Cardiovasculares (CIBERCV), Madrid, Spain

*Corresponding Author:

Jesús Lavado-García (e-mail: jesus.lavado@uab.cat)

ABBREVIATIONS

CDE: Cell Density Effect

DTT: Dithiothreitol

EDTA: Ethylenediaminetetraacetic acid

eGFP: enhanced green fluorescence protein

F17: FreeStyle F17™ cell culture media

FASP: Filter Aided Sample Preparation

Gag::eGFP: translational fusion of HIV-Gag protein and eGFP

hpt: hours post transfection

LC-MS/MS: Liquid Chromatography coupled with tandem mass spectrometry

MVB: Multi Vesicular Bodies

PBS: Phosphate-buffered saline

PEI: polyethyleneimine

PVDF: Polyvinylidene fluoride

RFU: Relative fluorescence units

ROS: Reactive Oxygen Species

SDS: Sodium Dodecyl Sulfate

SGE: Stable Gene Expression

TEAB: etraethylammonium tetrahydroborate

TFA: Trifluoroacetic acid

TGE: transient gene expression

THF: Tetrahydrofolic acid

TMT: Tandem Mass Tag

VLP: virus-like particle

ABSTRACT

The production of virus-like particles (VLP) has gained importance over the last few years owing to the benefits they provide compared to conventional vaccines. The biopharmaceutical industry is currently searching for safer candidates based on VLPs for new and existing vaccines and implementing new methods of manufacturing, thus allowing a more sustainable, effective and species-specific production. Despite achieving lower yields compared to traditional platforms, the use of mammalian cells provides the right post-translational modifications, and consequently, the intensification of bioprocesses using mammalian cells platforms has become a matter of pressing concern. One of the methods subject of intensification is transient gene expression (TGE), which has been proven to be highly effective regarding VLP production for preclinical or even clinical trials. In this work, a multiplexed quantitative proteomic approach has been applied to study the molecular characteristics of HEK293 cell cultures when growing at cell densities higher than $4 \cdot 10^6$ cells/mL, and the effects related to cell transfection and to VLP production. The obtained results revealed a set of functional and metabolic profiles of HEK293 under these three different conditions that allowed the identification of physiological bottlenecks regarding VLP production. Regarding the cell density effect (CDE), molecular alterations in the cell biology were proposed helping explain the difficulty for the cells to be transfected at higher densities. In addition, an overall disruption of cellular homeostasis after transfection was observed based on altered biological processes and after identifying potential pathways liable to be optimized via metabolic engineering, different solutions are proposed to improve VLP production.

Keywords: VLP, HEK293, HIV, transient transfection, cell density effect.

INTRODUCTION

The industry of biopharmaceutical manufacturing has widely adopted the use of animal cell cultures as the platform production due to the complexity of the biological products that are being used for new therapies. The eukaryotic cellular machinery catalyzes the correct folding of these macromolecular structures, coordinates the assembly of different subunits and incorporates post-translational modifications, essential for the final biomolecule to exert the proper biological function[1]. Recombinant subunit vaccines are one of the biopharmaceuticals produced in animal cell cultures currently growing in the market[2,3]. This approach is much safer and efficient than traditional vaccines built on live-attenuated or inactivated viruses containing no viral genetic material and thus, being non-infectious. Recombinant subunits of viral proteins have been used as vaccines since 1986 when the recombinant hepatitis B surface antigen (HBsAg) proved to auto-assemble into particles mimicking the native structure of the virus that had immunogenic capacity. Therefore, conferring immunity against the virus[4].

This is the beginning of the so-called Virus-like particles (VLPs). Since then, there has been a rapid increase in the development of new forms of production, designs for new antigens and new targeted viruses, becoming a potential platform for unprecedented therapies. One of these novel candidates is the Human Immunodeficiency Virus (HIV) whose core protein can undergo auto-assembly and coordinates to form a VLP. This core is formed by Gag polyprotein, which comprises six different parts: matrix protein (MA), capsid protein (CA), spacer peptides (SP1, SP2), nucleocapsid protein (NC) and p6[5]. The native HIV is an enveloped virus, meaning that it leaves the cell by budding, carrying with it part of the host cell membrane. In order to produce an enveloped HIV-1 VLP, the producer cell needs to express the gene coding for Gag polyprotein and allow cell budding. The cell machinery responsible for sending Gag to the membrane and for the later excision and release of the particles via budding is the endosomal sorting complexes required for transport (ESCRT)[6–10]. Two motifs from Gag p6 interact with TSG101 from complex ESCRT-I and ALIX (PDCD6IP)[11], the coordinator protein between ESCRT-I and ESCRT-III. This interaction leads to the recruitment of subunits of ESCRT-III[12] that are placed forming a ring that strangles the plasma membrane forming the new out coming enveloped particle[10]. ESCRT-III is the main responsible for excision[8]. The final step to release the new particle is carried out by the effector protein Vps4 which upon ATP hydrolyzation performs the cleavage[13]. The role of ESCRT-II is still uncertain as it appears it is not involved in HIV

budding[14] although some examples proving its requirement for the process have been shown[15]. Its role remains unclear. Alternative accessory proteins also play a role in sending Gag to the membrane. It is the case of the ubiquitin ligase NEDD4L[16–18]. Ubiquitinated proteins interact with domains of proteins from ESCRT-0 and might interact with ESCRT-II in the process of sending Gag to the membrane[19]. N-myristylation of Gag MA has also been reported to have targeting effects[6,11].

Mammalian cell lines like Chinese Hamster Ovary (CHO) or Human Embryonic Kidney 293 (HEK 293) are being exploited for this purpose thanks to their ability to produce recombinant proteins in suspension cultures upon transfection[20]. In order to achieve this, two main strategies have been developed, stable gene expression (SGE) and transient gene expression (TGE). SGE is based on the integration of the protein-coding gene in the genome while TGE relies on episomal DNA expression. While SGE is commonly used for well-established and characterized bioprocesses[21], TGE still prevails among previous stages of clinical trials due to the versatility of the technique, the need of performing different screening tests and the reduced costs of implementing TGE compared to SGE[22,23]. TGE involves transient transfection of the gene of interest, which enters the cell complexed by compounds like the cationic polymer polyethylenimine (PEI)[24]. The cell culture begins producing at around 2 hours post-transfection (hpt) and the product is further harvested between 48 and 72 hpt[25]. TGE has been described as a potent method of recombinant protein production[26] together with the use of HEK293 owing to the suitability of this cell line for transfection.

Although the implementation of TGE has been demonstrated at larger scale, where it has been reported to work at 100L scale in stirred tanks[27], it still remains predominant at preclinical stages since transfection yield decreases in mammalian cell cultures. This lower yields could be overcome via strategies involving transfection at higher densities. This presents important problems due to the cell density effect. Transfection is usually carried out at cell densities of $2 \cdot 10^6$ cells/mL and it is considered high cell density from $4 \cdot 10^6$ cells/mL up to higher orders of magnitude. If transfection is carried out when growing cells exceed $4 \cdot 10^6$ cells/mL, it becomes more difficult to successfully transfect them and the percentage of transfected cells abruptly decreases. Many strategies has been implemented to surpass this obstacle as diluting the cells to $2 \cdot 10^6$ cells/mL prior to transfection and changing the media to avoid spent media interference but the nature of problem remains unclear. Centrifuging cells at $2 \cdot 10^6$ cells/mL to concentrate before transfection proved to work[28] suggesting the referred cell density effect might be

related and conditioned by the intrinsic metabolic state of the cells. The same problematic appears when working with insect cell lines[29].

With the implementation of perfusion in bioprocessing productions, cell cultures are able to reach very high densities up to 50-150·10^6 cells/mL [30,31]. The rapid advances in the field are making essential the need to characterize metabolic bottlenecks regarding transfection and production and some insights of the metabolic causes of the cell density effect. This work has focused on the study of the changes in the HEK293 proteome when growing without transfection, when transfected with an empty plasmid and when transfected with Gag-coding gene to produce Gag VLPs, demonstrating the differential proteins changes in each cellular state. These findings will provide new keys for further metabolic engineering and optimization of VLP production.

MATERIALS AND METHODS

HEK 293 MAMMALIAN CELL LINE, CULTURE CONDITIONS

The cell line used in this work is a serum-free suspension-adapted HEK 293 cell line (HEK293SF-3F6) kindly provided by Dr. Amine Kamen from McGill University (McGill, Montreal, Canada). Cells were cultured in disposable polycarbonate 125 mL flasks with vent cap (Corning®) at 37ºC, 5% of CO_2 and 85% RH at 130 rpm in a LT-X Kuhner shaker (LT-X Kuhner, Birsfelden, Switzerland). Culture media was FreeStyle™ F17 Expression Media (Gibco, Life Technologies, ThermoFisher, San Jose, CA, USA) supplemented with 8 mM GlutaMAX™ (Gibco, Life Technologies, ThermoFisher, San Jose, CA, USA), 0.1% Pluronic™ F-68 Non-ionic Surfactant (Gibco, Life Technologies, ThermoFisher, San Jose, CA, USA) and IGF-1 at a final concentration of 50μg/L.

Cell counts and viability were performed using the NucleoCounter®NC-3000 automatic cell counter (Chemometec, Allerod, Denmark) according to manufacturer's instructions.

Glucose and lactate were measured using YSI 2700 select glucose/lactate analyzer (YSI, Yellow Springs, OH, USA) according to manufacturer's instructions.

TRANSIENT TRANSFECTION

Transfections were carried out at a cell density of $2 \cdot 10^6$ cells/mL using a final DNA concentration of 1 μg/mL. PEI/DNA complexes were formed by adding PEI to plasmid DNA diluted in fresh culture media (10% of the total culture volume to be transfected). Transfection reagent PEIpro® (Polyplus-transfection, Illkirch-Graffenstaden, France) was used.

The plasmid used contained a gene coding for HIV-Gag protein fused in frame to eGFP (Gag::eGFP). This is a translational gene fusion of HIV-*gag* gene and *egfp* gene under a CMV enhancer and CMV promoter with no IRES sequence between them. Briefly, pGag::eGFP plasmid was diluted with supplemented FreeStyle™ F17 media and vortexed for 10 seconds. Then PEI was added in 1:2 (w/w) DNA:PEI ratio and vortexed three times, then the mixture was incubated for 15 min at room temperature and added to the cell culture.

FLOW CYTOMETRY

Samples were taken at each time point and cells were fixed using formaldehyde 2% during 10 minutes, centrifuged and then resuspended in PBS for FACS analysis. The percentage of GFP positive cells was assessed using a BD FACS Canto flow cytometer (BD Biosciences, San Jose, CA, USA). Laser 488 was used for GFP measurement. The results were analyzed with FACS DIVA software (BD Biosciences, San Jose, CA, USA).

HIV-1 GAG VLP QUANTIFICATION

The concentration of HIV-1 Gag VLPs was assessed by fluorimetry using an in-house developed and validated quantification assay[32]. VLP containing supernatants were recovered by cell culture centrifugation at 1000×g for 5 min. Relative fluorescence unit values (RFU) were calculated by subtracting fluorescence unit (FU) values of non-transfected negative control samples. There is a linear correlation between fluorescence intensity and p24 values determined using the INNOTEST ELISA HIV antigen mAb (Innogenetics NV, Gent, Belgium). RFU values can be converted to Gag::eGFP concentration values using the following equation:

$$\text{Gag::eGFP (ng/mL)} = (3.245 \times \text{RFU} - 1.6833) \times 36 \qquad (1)$$

where Gag::eGFP is the estimated concentration of polyprotein and RFU is the measured GFP fluorescence intensity in the samples. The first term is the correlation equation between fluorescence values and p24 concentrations determined by ELISA and 36 is a correction factor that takes into account the difference in molecular weight between p24 and Gag::eGFP and an underestimation arising from using the p24 ELISA to estimate p55 Gag concentrations. Assuming that a single VLP contains 2,500 Gag::eGFP molecules[33] and that one Gag::eGFP is 84kDa ($1{,}39 \cdot 10^{-10}$ ng), the concentration of VLPs can be calculated.

PROTEIN SAMPLES PREPARATION FOR MASS SPECTROMETRY ANALYSES

Pellets of each tested condition were obtained by centrifugation of 500 μL of the cell culture at 10000xg for 15 minutes at 4ºC. Pellets were stored at −80ºC.

Protein extraction was performed using extraction buffer (100 mM Tris-HCl pH=8.8, 2mM EDTA, 4% SDS, 100mM DTT) of which 100μL were added to the cell pellet of each condition. Samples were sonicated for 5 minutes and then boiled for another 5 minutes. Protein extracts from pellets samples were quantified with RC/DC Protein Assay (Bio-Rad, Hercules, CA, USA) and stored in -20 ºC until the tryptic digestion process. Protein digestion was performed as previously described[34]. Proteins were digested using sequencing grade trypsin (Promega, Madison, WI, USA) and the filter-assisted sample preparation technology (FASP, Expedeon, San Diego, CA, USA), and the resulting peptides were subjected to TMT-10 plex labelling (AB Sciex, Framingham, MA, USA), joined and desalted.

A total of 150μg from samples of each condition was diluted to a final concentration of 100mM of TEAB labeled with TMT-10 plex according to the manufacturer. Protein samples were labeled by adding 41μL of TMT isobaric tag diluted in anhydrous acetonitrile, followed by a 1h-incubation step at room temperature. To quench the reaction, 5% hydroxyl-amine (8μL per sample) was added, incubated 15 min at room temperature and mixed together followed by addition of TFA 1% to lower pH at 3. TMT-labeled samples were equally mixed. Pooled mix was purified using Oasis HLB C18 column (Waters, MA, USA).

TMT-labeled mix was fractionated using High pH reversed-phase peptide fractionation kit (Thermo Scientific, San Jose, CA, USA) according to manufacturer's instructions into 5 fractions for further LC-MS/MS analysis.

LIQUID CHROMATOGRAPHY TANDEM MASS SPECTROMETRY ANALYSIS

The tryptic peptide mixtures were subjected to LC-MS/MS analysis on a ano-HPLC Easy nLC 1000 liquid chromatograph (Thermo Scientific, San Jose, CA, USA) coupled to a QExactive mass spectrometer (Thermo Scientific, San Jose, CA). Peptides were suspended in 0.1% formic acid, loaded onto a C18 reverse-phase trapping column (Acclaim PepMap100, 75-μm internal diameter, 3-μm particle size and 2-cm length, Thermo Scientific), and separated on an analytical C18 nano-column (EASY-Spray column PepMap RSLC C18, 75-μm internal diameter, 3-mm particle size and 50-cm length, Thermo Scientific), in a continuous gradient (8–31%B in 240 min, 31–90%B in 2min, 90%B in 7 min, and 2%B in 30min; where buffer A is 0.1% formic acid in HPLC grade H_2O and buffer B is 100% ACN, 0.1% formic acid in HPLC grade H_2O). Spectra were acquired using full ion scan mode over the mass-to-charge (m/z) range 390–1500, 70,000 FT-resolution was performed on the top 15 ions in each full MS scan using the data-dependent acquisition mode with 45s dynamic exclusion enabled.

PROTEIN IDENTIFICATION AND QUANTIFICATION

Protein identification was performed over the raw files using the SEQUEST HT algorithm integrated in the Proteome Discoverer 2.1 (Thermo Finnigan). MS/MS scans were matched against a human database (UniProtKB/Swiss-Prot 2017_10 Release). Sequence of Gag::eGFP protein was added to the selected database to enable identification.

For database searching, parameters were selected as follows: trypsin digestion with 2 maximum missed cleavage allowed, precursor mass tolerance of 800 ppm, fragment mass tolerance of 0.02 Da. TMT-10 plex labeling at N-terminal and lysine (+229.62932 Da) as well as cysteine carbamidomethylation (+57.021 Da) were chosen as static modifications whereas methionine oxidation (+15.994915 Da) was chosen as dynamic modification. The same

MS/MS spectra collections were searched against inverted database constructed from the same target database. SEQUEST results were analyzed by the probability ratio method[35]. False discovery rate (FDR) for identified peptides was calculated in the inverted database search results using the refined method[36].

Quantitative information of TMT reporter ions was extracted from MS/MS spectra for relative quantification of protein abundance to characterize dynamic protein expression profiles in the selected conditions.

STATISTICAL ANALYSIS

For the comparative analysis of the protein abundance changes we applied Weighted Scan- Peptide-Protein (WSPP) statistical workflow[37,37], using SanXoT package[39]. It uses as an input a list of quantifications in the form of log2-ratios (for example a condition versus control sample) with their statistical weights and generates the standardized forms of the original variables computing the quantitative values expressed in units of standard deviation around the averages. The quantitative information is obtained from the spectra and used to quantify the peptides from which the spectra are produced and then, proteins that generate these peptides. In other words, the quantitative information is integrated from the spectrum level to the peptide level and then from the peptide level to the protein level[40]. These standardized variables, (Zq), express the quantitative values in units of standard deviation[41]. For the protein functional analysis, Systems Biology Triangle (SBT) model[42] was used. This algorithm estimates weighted functional category averages (Zc) from the protein values by performing the protein to category integration. After the integration from spectra to peptide, this integration represent a higher level, from peptide to category. This integration allows the detection of changes in functional categories produced by the coordinated behavior of their proteins[40]. The quantified proteins were functionally annotated using the Gene Ontology database[43,44]. For further Gene Ontology annotation, DAVID[45,46] was used to perform functional enrichment analysis and to extract *p-values* for the enriched processes. To help analyze and comprehend the data, the online software for reactions, proteins and pathways analysis REACTOME[47] was used.

WESTERN BLOTS

RC/DC protein quantification was used to normalize protein used for western blot. A total of 20μg of each condition was separated on SDS-PAGE and transferred onto a polyvinylidene difluoride (PVDF) membrane for 7 minutes using the system Trans-Blot® Turbo™ Transfer System (Bio-Rad, Bio-Rad, Hercules, CA, USA) as described in the instructions. Membranes were incubated overnight with diluted primary antibody in 5% (w/v) non-fat dry milk 1x TBS 0.1% Tween-20 at 4ºC with gentle shaking. Primary antibodies used for protein validation were anti-Histone

H2A antibody (L88A6, Cell Signaling Technology, 1:1000), anti-Histone H3 antibody (96C10, Cell Signaling Technology 1:1000), anti-Importin4 antibody (ab181037, Abcam, UK, 1:10000), anti-HMGCS1 antibody (ab155787, Abcam, UK, 1:3000), anti-ACSF2 antibody (ab180068, Abcam, UK, 1:1000), mouse Anti-TSG101 antibody (612696, BD Biosciences), mouse monoclonal antibody to HIV-1 p24 (A2-851-100, Icosagen, Estonia, 1:1000). After primary incubation, a secondary incubation was performed using anti-Rabbit IgG coupled with alkaline phosphatase antibody produced in goat (A9919, Sigma Aldrich, San Luis, MO, USA) and anti-Mouse IgG coupled with alkaline phosphatase antibody produced in goat (A3562, Sigma Aldrich, San Luis, MO, USA) as required in 2.5% (w/v) non-fat dry milk 1x TBS 0.1% Tween-20 for 1 hour at room temperature. Proteins were visualized using NBT-BCIP® solution (Sigma Aldrich, San Luis, MO, USA) incubating the membrane for 2-3 minutes. Membranes were let to dry and then scanned at 400 bpi and analyzed using the software ImageJ[48].

EXPERIMENTAL DESIGN

For the multiplexed quantitative proteomics experiment based on TMT-10 plex labeling, three conditions were tested in this study: no transfection (N) transfection with empty mock plasmid (M) and transfection following the standard protocol (S) previously described. The mock plasmid shares the same backbone as the plasmid coding for Gag::eGFP but lacks the whole *gag::egfp* gene. Samples of each condition were taken at 2 hours post-transfection (2 hpt) and 72 hours post-transfection (72 hpt). As it is depicted in **Figure 1A**, the TMT-based isobaric labelling quantification was performed with three biological replicates for each condition. A peptide pool from the non-transfected condition at 2hpt was used as an internal control for the following statistical analyses.

RESULTS

The following analyses are described using the following notation: non-transfected condition (**N**), mock condition (**M**) and standard Gag::eGFP transfected condition (**S**). The standardized log2-ratios (from analyzed condition versus the internal control) measured in units of deviation (**Zq**) was used to perform the following analyses. The same type variable but at the level of functional category was also used (**Zc**).

Cell culture growth, VLP production and quantification

Cell cultures were inoculated at $0.5 \cdot 10^6$ cells/mL and transfected when reached $2 \cdot 10^6$ cells/mL. As shown in **Figure 1B**, after transfection (at time point 0), transfected conditions (M and S) stopped cell growth and maintained their concentration at $2 \cdot 10^6$ viable cells/mL while cell viability started to slightly decrease from 98% to 78% at 72 hpt.

Conversely, the non-transfected control condition (N) continued growing reaching $6 \cdot 10^6$ cells/mL at 72 hpt maintaining viability at 96%. Both M and S conditions behave similarly, regardless of the nature of the plasmid that the cells have been transfected with. To monitor transfection, samples of each time point from the conditions transfected with pGag::eGFP were analyzed by flow cytometry to quantify the percentage of GFP positive cells. At 72hpt cells reached the highest percentage of transfection (*p-value* = 0.02*)* with 95% of GFP positive cells as shown in **Figure 1C**. Production of VLPs was assessed by fluorimetry and converted to VLP concentration (VLP/mL) using an in-house developed protocol[32]. **Figure 1D** shows the significant increase (*p-value* = 0.0002) of particle production from 24 to 48 hpt and were harvested at its maximum at 72 hpt when particle concentration reached $1.6 \cdot 10^{10}$ VLPs/mL.

Transfection at different cell densities was tested from 2 to $5 \cdot 10^6$ cells/mL. Transfection efficiency dramatically decreases if transfection is performed at cell densities higher than $3 \cdot 10^6$ cells/mL. When transfected at $2 \cdot 10^6$ cells/mL, transfection efficiency reaches 92% at 72hpt whereas if transfected at $4 \cdot 10^6$ cells/mL, percentage of transfection drops to 3%. Transfection was already reduced at $3 \cdot 10^6$ cells/mL, hindered at $4 \cdot 10^6$ cells/mL and completely inhibited at $5 \cdot 10^6$ cells/mL (**Figure 1E**), even using media able to sustain cell densities of $7\text{-}8 \cdot 10^6$ cells/mL where glucose was maintained above 1g/L up to 5 days of culture (**Figure 1F**). The same effect was observed using HyCell™ TransFx-H (HyClone) media (**Supplementary Figure S1**).

Proteomic characterization of HEK293 at 2 and 72 hours post HIV-1 Gag transfection

A comparative analysis of the HEK293 cell proteome without transfection, transfected with an empty plasmid and transfected with the plasmid containing the gene *gag::egfp* at 2 and 72 hours post transfection as carried out by high-throughput multiplexed quantitative proteomic analysis. A total of 7262 proteins were identified and quantified in this study (FDR < 0.01), with 4403 proteins quantified with more than one peptide (**Supplementary Table S1)** and 3335 shared in both time points (**Figure 2A**).

The functional enrichment analysis performed on the 667 unique proteins (**Figure 2B**) found at 2hpt confirmed that at that time point the most significant biological process is protein transport (*p-value* = $7.2 \cdot 10^{-8}$*)*. However, this enrichment was not due to Gag production since no Gag::eGFP was detected at 2hpt (**Figure 2D**). At 2hpt, the DNA/PEI complexes are still being taken up by the cell and transported to the nucleus but no expression of *gag::egfp* is yet detected[49]. Another significantly enriched biological processes were proteasome-mediated

ubiquitin-dependent protein catabolic process, establishment of protein localization, protein ubiquitination and protein K63-linked deubiquitination. A similar enrichment analysis was performed on the unique 401 proteins found at 72hpt. Coherently, at this time point, when VLPs are being produced, Gag::eGFP is detected by western blot (**Figure 2D**). Gag::eGFP is the quantified protein showing the highest significance (FDR=0). The significantly enriched biological processes found are related to the secretion of proteins into the extracellular space and cell division, such as regulation of small GTPase mediated signal transduction, endocytosis, cytoskeleton-dependent intracellular transport, microtubule-based movement and chromosome segregation (**Figure 2C**). Interestingly, the endocytosis process is related to the formation of the Multi Vesicular Bodies (MVB) component, which allows intracellular budding of VLPs[50] and later cell release as exosomes.

To further characterize the differences between 2 and 72hpt, proteins and processes were grouped depending on their up or downregulation at each timepoints (**Figure 2E**). Proteins were selected with Zq greater or equal than 1.5 for upregulations and lower or equal than -1.5 for downregulations. Processes identified and quantified with more than 4 proteins were selected with Zc greater or equal than 1.5 for upregulations and lower or equal than -1.5 for downregulations. It can be drawn from this analysis that 86% of all altered processes are identified and quantified at 72hpt. Regardless of the studied condition, there is a clear molecular and metabolic shift that is taking place from 2 to 72hpt.

These results are an overall view of the initial and final state of HEK293 cells along the transient transfection time course, albeit more detailed analyses can be drawn out focusing on individual protein changes in each condition. Protein up and downregulations presented in all three conditions (N, M and S) were attributed to cell growth, regardless of transfection, providing insight of the metabolic alterations that could be found in HEK293 cultures growing at high cell density. Changes presented in each transfected condition, regardless of the plasmid used, could be explaining the transient transfection process. Finally, changes found only in the condition transfected with the plasmid pGag::eGFP could be deciphering the effect of VLP production on the cell physiology. The next analyses were carried out following these guidelines.

Proteomic analysis of HEK293 cell growth

Proteins showing a common pattern of alteration in all three conditions comparing the time points 2 and 72hpt using Zq, were classified in four groups such as transport proteins (importins and exportins), lipids and metabolites

biosynthesis, mitochondrial and histones proteins. **Figure 3** shows protein abundance changes (Zq) of all the proteins showing the same alteration in all conditions. In **Figure 3A** it can be observed that the four selected group of proteins are the ones showing the highest significance and greatest abundance changes. All identified importins showed a downregulation at 72hpt mainly indicated by importin subunit alpha-1, 8 and 4, importin-11, importin-5 and importin-4. Moreover, all identified exportins also presented downregulation at 72hpt from which exportin-T, exportin-1 and exportin-2. Lipids and metabolites biosynthesis also showed downregulation at 72hpt. Proteins like fatty acid synthase, cytoplasmic hydroxymethylglutaryl-CoA synthase, squalene synthase, glutamine synthetase, ATP-citrate synthase, thymidylate synthase and up to 18 biosynthesis related enzymes showed a significant decrease at 72hpt. Likewise, an increase in mitochondrial protein composition can be found at 72hpt. Up to 30 mitochondrial proteins presented upregulation compared to 2hpt (**Figure 3A**). A more significant increase appeared in the non-transfected condition (N). In addition to this, histones and histones-related proteins like non-histone chromosomal protein and histone lysine-methyltransferases were also significantly increased at 72hpt. Validation of relevant and representative proteins of each group were performed using western blot (**Figure 3B**). It is illustrated in **Figure 3C,** showing the up and downregulation of proteins like ACSF2 (mitochondrial protein), HMGCS-1(lipid biosynthesis), IPO4 (nuclear import transport), H3 and H2A (nucleosome).

Proteomic analysis of HEK 293 transfection

Upon transfection, cellular viability starts decreasing (**Figure 1B**). A broader overview of the changes in cell physiology upon transient transfection is listed in **Figure 4**. Unlike the changes related to the cell density effect, transfection seems to influence homeostasis in the entire cell, affecting a wide range of pathways. This systemic alteration was analyzed using biological processes GO terms. At 72 hours post transfection, there was an overall decrease in several metabolic and physiological processes, as approximately 79% of all analyzed processes were downregulated (**Figure 4C**). The upregulated processes corresponded to the remaining 21%, involving gene expression, protein production and microvesicles/exosomes machinery activation. Interestingly, both ER and cytosolic ribosome protein translation were upregulated. Regarding exocytosis, protein trafficking towards the cell membrane was pointed out in the analysis as GO terms such as phosphatidylinositol-4, vesicle docking and the cytoskeleton are increased (**Figure 4A**). This suggested that the network cytosolic protein production and ER-Golgi network trafficking were both enhanced upon transfection.

Curiously, there was a group of processes that not only were downregulated upon transfection, but also increased in the non-transfected condition (N) at 72hpt compared to 2hpt (**Figure 4D**), suggesting that transfection prevented cells from upregulation interfering especially in these processes. Coherently to the phenomena observed in **Figure 1B**. The complexation agent (PEI) used for transfection prevents cell growth due to its cytotoxic effects. Therefore, processes related to DNA regulation are downregulated upon transfection. DNA repair, nuclear chromosome formation and histone exchange were downregulated. Metabolic processes such as glycosphingolipid metabolism and NADP+/ADP ribosyltransferase activity also belong to this group of altered processes. The rest of downregulated processes indicated in **Figure 4** cover some homeostatic pathways mostly related to detoxification and damage repair. Homeostasis is disrupted at different levels. At DNA level, processes like DNA binding, mismatch edition or telomere maintenance were downregulated. At enzyme level, many metabolic enzymes whose function depend on metal ion binding such as Co^{2+} binding, THF, pyrimidines or xenobiotic binding and detoxification were decreased. Peptidase activity is reduced as well. Redox homeostasis is also disrupted. Glutathione-related processes like glutathione biosynthesis, reductase activity, dehydrogenase activity, and glutathione binding are decreased. Cell signaling and the response to stimulus also appeared to be altered since Ca^{2+} binding proteins, Ca^{2+}-related processes like Ca^{2+} sequestration, release, regulation, channel localization and ryanodine receptors involved in signaling pathways, all showed downregulation at 72hpt in transfected conditions compared to non-transfected ones.

Proteomic analysis of HEK293 VLP production

HIV-Gag VLPs were successfully identified being Gag::eGFP is the protein identified with the highest intensity in the whole study. Regarding cellular physiology, compared to the alterations observed after transfection, VLP production had a minor effect on cell physiology (**Figure 5)** compared to the homeostatic alterations due to transfection. The most remarkable change was the increase of Gag::eGFP protein at 72hpt while the rest of the proteins showing alterations were only detected at 2hpt. Within these altered proteins, two groups were observed. The first group were proteins upregulated in conditions non-transfected (N) and transfected with mock plasmid (M) while showing no change in VLP-producing condition (S). Belonging to this group, ubiquitin ligases of RNF family and accessory proteins like Sharpin were found. Cell adhesion and proteins relevant in the extracellular matrix composition like protocadherin and collagens were also altered. The second group is formed by proteins showing

downregulation in S compared to the rest. Similar proteins as the ones found in the previous group, were also found here. Different ubiquitin ligases from RNF family, transcription repressors, zinc fingers, Ca^{2+} -dependent proteins and voltage channels were present. There were no significant processes showing upregulation when producing VLPs.

The ESCRT machinery

The machinery responsible for processing and secreting Gag-based VLPs is the one comprising the ESCRT complexes[8]. The heat map of all ESCRT proteins in the different conditions at 2 and 72hpt is shown in **Figure 6A**. All ESCRT proteins were identified and quantified. However, no significant changes were observed regarding the components of the ESCRT complexes comparing 2 and 72hpt. Although no protein showed individual significant increase or decrease, the overall variation of the whole ESCRT-I showed a significant decrease (p-value < 0.0001) from 2 to 72hpt, showing a coordinated behavior of all of its proteins (**Figure 6B**). ESCRT-II and ESCRT-III complexes did not show significant variations. Variation of TSG-101 was assessed by western blot and showed no significant difference from 2 to 72 hpt (**Figure 3C**) validating the previous results.

Accessory proteins like NEDD8 and NEDD4L ubiquitin ligases, also important for sending Gag to the cell membrane and promoting cell budding were quantified. Interestingly, at 72hpt this group of proteins were found to be significantly downregulated.

DISCUSSION

The Cell Density Effect (CDE)

Regardless of any external distress, the mere cell growth influences the metabolic and physiological state of the cell affecting the later processes of transfection and production. It has been widely reported that productivity in cell cultures decreases when transfection is carried out at higher cell densities[29,51–53]. This phenomenon is known as Cell Density Effect (CDE). It affects different production approaches: transfection[54], infection[29], mammalian[52,53,55] and insect cells[56]. The limitation imposed by this constraint prevents the production process from being thoroughly exploited when scaled up. If cultures need to be maintained at early exponential phase ($1\text{-}2\cdot10^6$ cells/mL) to be effectively transfected, the potential of scaling up is reduced[57]. During the last decade different studies regarding

the CDE has been conducted and showed some metabolic variations in high cell density cultures, mostly regarding energy[53,56,58]. CDE was thought to be mainly a metabolic issue, concerning the limited resources available when high concentrations of cells are reached. ATP was described to help attenuate the CDE[59] as perfusion cultures started to be implemented[30] since a continuous addition of fresh media provides the necessary source of carbon, preventing glucose from depletion and maintaining ATP production. However, when carrying out transient transfection at high cell densities operating in perfusion mode, difficulties to transfect the cells still appeared[60]. Encountering the CDE in perfusion mode suggests that molecular mechanism are influencing this phenomenon beyond energetic issues and media depletion is not a determining factor in the CDE. Cell division requires energy and gene expression. As cells reach high densities along with cells which are recovering from a cytotoxic event like transfection, the need of energy increases. Our results showed an upregulation of histones, chromosomal proteins, gene expression and mitochondrial components that reflects the increase in energy demand and it is intimately related to the CDE. However, energy is not the only element behind the CDE and different physiological causes remain unknown[53]. Using media able to sustain densities of 10^7 cells/mL, the same effect was observed at 3-4·10^6 cells/mL, suggesting there are more cellular processes playing a role rather than being only an energy issue. Maintaining glucose above 1g/L in the conditions where a decrease in transfection efficiency was observed indicates that energy depletion is not a limiting and influencing factor.

In addition to this, how the cell cycle affects transfection efficiency was already reported[25] and showed that when transfecting HEK293 at high cell densities cell cycle does not present a limiting factor and does not influence the difficulty found to achieve high transfection efficiency. Still, no molecular contribution has been reported so far regarding this issue. This study helps cast some light on some molecular mechanisms that are being altered at densities above 4·10^6 cells/mL which are strongly related to the event of transfection and processing of the exogenous DNA. When DNA/PEI complexes are added for transfection, they first encounter various cell membranes until they reach the nucleus, where the plasmid stays as episomal DNA[49]. To be able to be transported into the nucleus the machinery of nuclear importin/exportin play a crucial role. DNA binds to importins and only then is able to cross the nuclear pores, following the unbinding of DNA/importing complex coupled with the hydrolysis of GTP into GDP[61]. Exportins work similarly transporting cargos from the nucleus to the cytoplasm. The downregulation of the whole nucleus transport machinery (exportins and importins showed in **Figure 3**) at high cell densities might explain the decrease of transfection efficiency and thus be a relevant component of the CDE. Our

work showed an essential component of the plasmid up taking pathway hitherto omitted in similar studies. Not only the energy balance is important to describe and characterize this effect, but also molecular mechanisms affecting the cell biology.

Another important factor is the decrease in lipid biosynthesis. A change in the lipid composition of the cell membrane might be essential to prevent the DNA/PEI complexes from entering the cell and block transfection. In addition, budding from the cell membrane is the secretory pathway used by HIV-VLPs and therefore for this platform. This implies a continuous remodeling and regeneration of the cell membrane to be able to cope with the constant production and release of VLPs. If the overall lipid biosynthesis is reduced, cells that recently acquired the plasmid might not engage in producing VLPs and cells that already are producing could start to slow the production rate. This, coupled with cell division and the subsequently loss of the plasmid will concur in a decrease of productivity from 72hpt along time[25].

Physiological consequences upon transfection

Transient transfection is a well-defined cytotoxic event. The addition of DNA/PEI complexes have proved to reduce cellular viability[62]. To avoid this problem, optimization strategies need to be found to improve PEI-mediated transfection[63]. Cytotoxicity of PEI has already been described[64]. However, the physiological cause wreaking havoc on cell culture viability still remained undescribed. Here, several altered biological processes have been identified showing homeostasis disruption and casting some light on the reasons for the cell viability to be reduced. Glycosphingolipid biosynthesis has previously been reported to increase during cell growth and even described as one of the metabolic causes of the cell density effect[53,65]. In non-transfected conditions, glycosphingolipid metabolic processes significantly increase. Yet upon transfection it is hindered. Glycosphingolipids act in the intracellular vesicle trafficking to promote cholesterol trafficking from cytosol to the membrane[66]. It is reported that its loss from the cytosolic cell membranes and lipid rafts alter vesicle trafficking[67] and the correct cholesterol transport and consequently correct lipid metabolism[68]. Interestingly, this cholesterol homeostasis disruption coincides with the downregulation of lipid biosynthesis previously described. The loss of relevant lipids from the cell membrane and the loss of lipid trafficking and lipid homeostasis prevents the cell from displaying a healthy signaling to the rest of the cell population[69] and more importantly, it alters essential physiological processes, contributing to the reduction of cellular viability. Glycosphingolipid metabolic process category comprises proteins like prosaposin, beta-hexosaminidase, sphingomyelin phosphodiesterase and acid ceramidase among others. This suggests that

breaking down ceramide and ceramide-derived lipids is blocked after transfection. Consequently, the release of fatty acids and other lipids from their glycosphingolipid precursors is hampered. Enhancing these pathways or adding fatty acids and other lipids, like cholesterol, when transfecting may clear this metabolic bottleneck. An additional approach in order to improve cell homeostasis upon transfection could be overexpressing enzymes promoting glycosphingolipids metabolism. An improvement in cellular homeostasis could enhance VLP production and grant the acquisition of higher protein titers.

Another important factor for cell survival is maintaining redox homeostasis. DNA/PEI complexes are highly charged molecules which when entering the cell modify cytosolic compartment polarization as calcium-dependent processes happen to be altered. The change in intracellular polarization is crucial for the right protein signaling and protein-protein interaction. Polarization changes also affects the mitochondria which can consequently alter energy homeostasis and increase reactive oxygen species (ROS)[70] damaging the cell. Curiously, proteins helping detoxifying the cell from ROS such as glutathione are also downregulated therefore suggesting redox homeostasis disruption caused by DNA/PEI complexes also contributes to decrease cellular viability. These series of changes may affect protein integrity, nevertheless some peptidases were also found to be decreased, hampering correct protein degradation. Accumulation of harmful undegraded proteins present a high risk for cellular homeostasis. Although PEI could be detoxified by the cell, this general homeostasis and protein disruption also affects xenobiotics catabolic processes, as well hindered.

Homeostasis disruption might not be the only cause for cellular viability to decrease upon transfection. Exogenous DNA might be also playing a role. Cellular machinery to repair, modify and bind DNA was downregulated. These processes are essential for DNA renewal in exponentially growing cells. If the cell cannot use this sort of mechanisms, it will find solutions for DNA detoxification. All of the biological processes found to be upregulated upon transfection point to the biosynthesis and release of exosomes. Interestingly, the production of exosomes has recently been described as a powerful mechanism of excreting DNA from the cell[71]. Upon a homeostasis-disruptive event, the cell engages mechanisms to eliminate the source of cellular stress generation. This upregulation in exocytosis suggests that DNA/PEI complexes could be being excreted via exosomes production in order to maintain homeostasis.

Physiological consequences of producing HIV-1 VLPs

Cells transfected with pGag::eGFP plasmid shared all previously described physiological effects caused by transient transfection. However, when cells start producing VLPs, they display some specific physiological changes related to the expression of episomal DNA and remodeling of the membrane proteins. At this scenario, most of the cell resources are being used either to fight homeostasis disruption or to produce VLPs. This translates into the downregulation of production and release of growth-signaling proteins. Cell communication is essential and VLP-producing cells need to focus their resources on surviving and producing so cell growth is slowed down. Production requires DNA expression, so specific zinc fingers, transcriptional repressors and DNA regulators were found downregulated, allowing expression of the exogenous DNA. There were not upregulated ribosomal processes, indicating that the cell does not enhance protein synthesis pathways, but instead, uses the constitutive protein synthesis activity to channel production towards VLPs. This might be the first bottleneck in VLP production that can be found. After the monomers of Gag are produced, they need to be sent to the membrane for assembly. The phase of sending Gag monomers to the membrane and their assembly is really important to determine physiological bottlenecks for the following optimization and improvement of VLP production. Previous work has already reported that the limiting step in VLP production is the transport of Gag monomers to the cell membrane[49] but the responsible molecular elements remained unknown. In this work, a close analysis of the ESCRT molecular pathway has been performed in order to identify the limiting step. The comparative of the different ESCRT complexes at 2 and 72hpt indicates that ESCRT-I presents a bottleneck in VLP production. ESCRT-I is responsible for sending Gag to the membrane[8,9] and at 72hpt showed an overall downregulation. This indicates that Gag is being produced but is not being sent to the cytoplasmic membrane at its fullest capacity. No alteration of ESCRT-II and ESCRT-III imply that even if it is not presenting any hindrance, it can be further optimized if any upregulation is achieved. In order to tackle this issue, accessory proteins like NEDD8 and NEDD4L which were found downregulated at 72hpt could be overexpressed to promote transportation of Gag to the membrane and enhance cell budding. Another possibility to improve VLP production is to promote intracellular budding. Biological processes like endocytosis or late endosomal-related pathways were quantified at 72hpt. VLPs are described to be produced also by intracellular budding[50,72] and overexpressing proteins like Citron-Rho Kinase could be a solution to promote this pathway. Once VLPs are being produced, secreted from the cell membrane, they take part of it with them during excision. VLPs are charged particles, meaning their constant production will interfere with cell membrane polarization, altering Ca^{2+} import. More interestingly, Ca^{2+} has been described to play an

important role regarding the multivesicular bodies (MVB) pathway, also leading to VLP intracellular budding. The downregulation in Ca^{2+} import observed when producing VLPs can be overcome by adding Ca^{2+} together with ionomycin, improving VLP production via intracellular budding by eight fold[73]. The combination of Citron-Rho kinase overexpression and the addition of free intracellular calcium and ionomycin could help increase VLP budding. Collagens and other extracellular proteins were as well altered, suggesting extracellular matrix composition itself is being modified along VLP production. Specific ubiquitin-ligase downregulated activity at 2hpt might indicate that ubiquitination is being redirected to a few processes, which could be directly related to Gag trafficking to the membrane.

CONCLUSIONS

Increasing the knowledge of cell physiology is key to understand and characterize the bioprocess that is trying to be optimized. The cellular causes for some well-known and observable effects in animal cell bioprocessing still remain not fully understood. In this work, some physiological causes are identified related to the cell density effect, the reduction of cell viability upon transient transfection and VLP production. A summary of the altered processes in each condition is shown in **Figure 7.**

The difficulty to achieve transfection when it is carried out at cell densities greater than $4 \cdot 10^6$ cells/mL is known as the cell density effect. This is partially explained by a downregulation in lipid biosynthesis and intracellular protein transport to the nucleus. Transient transfection depends on the physiological state of the cells and thus it is directly related to cell density. The decrease in cellular viability upon transfection is caused by a systemic disruption of homeostasis due to many levels of homeostasis control being altered, such us glycosphingolipids metabolism, calcium regulation, oxidant detoxification, xenobiotic metabolism, peptidases activity and DNA detoxification. When producing VLPs, these traits are maintained and specific modifications in the extracellular matrix and membrane calcium channels are evidenced.

These findings could support designing less stressful processes enabling the productivity to increase, to reduce bottlenecks and help establish fundamental cell physiological basis for future, more effective bioprocesses.

SUPPORTING INFORMATION

The following supporting information is available free of charge at ACS website http://pubs.acs.org

Supplementary Figure S1: Decrease in transfection efficiency at high cell density in HyCell™ TransFx-H media.

Supplemetary Table S1: List of all Identified proteins in this study.

FUNDING

The project that gave rise to these results received the support of a fellowship from ”la Caixa” Foundation (ID 100010434). The fellowship code is LCF/BQ/ES17/11600003. This study was supported by competitive grants from the Spanish Ministry of Economy and Competitiveness (MINECO) (BIO2015-67580-P, PGC2018-097019-B-I00) through the Carlos III Institute of Health-Fondo de Investigación Sanitaria (PRB3, PT17/0019/0003 ISCIII-SGEFI/FEDER) and by CIBERCV (CB16/11/00277). The CNIC is supported by the Ministerio de Ciencia, Innovación y Universidades and the Pro-CNIC Foundation, and is a Severo Ochoa Center of Excellence (SEV-2015-0505).

DATA AVAILABILITY

The raw mass spectrometry data has been submitted to the ProteomeXchange Consortium (http://proteomecentral.proteomexchange.org) with the dataset identifier PXD014746.

AKNOWLEDGMENTS

The authors thank Dr. Amine Kamen (McGill University, Montreal, Canada) for providing the HEK 293 SF-3SF6. The following reagent was obtained through the National Institutes of Health AIDS Reagent Program, Division AIDS, National Institute of Allergy and Infectious Diseases, National Institutes of Health: pGag::eGFP (Cat#11468) from Dr. Merilyn Resh.

FIGURE LEGENDS

Figure 1. Experimental design and cell growth and VLP production data. **A)** Experimental workflow. Three biological replicates of HEK293 cells were cultured in three different conditions. No transfected condition, transfected with an empty plasmid denoted as 'mock' and transfected using the standard protocol with the plasmid containing the gene gag::egfp gene. Both transfections were performed at the same cell density of $2 \cdot 10^6$ cells/mL. At the time point of 2 hours post transfection (hpt) cultured samples were taken, centrifuged and cellular pellets were stored at -80ºC. Same procedure was repeated at 72hpt. Proteins were extracted from the pellet samples, digested and peptides were labelled using Tandem Mass Tag (TMT) labelling. Labelled peptides were fractionated and analysed via LC-MS/MS. **B)** Viable cell density and cell viability graphs along the time course. The red dotted line indicates 50% of cell viability. Cells were transfected at time point 0. **C)** Flow cytometry analysis of the transfection percentage (showed in GFP positive percentage of cells) in the different conditions along the time course. **D)** VLP concentration in the supernatants of the standard transfection condition along the time course, showing the production of VLPs. **E)** Flow cytometry analysis of the transfection percentage (showed in GFP positive percentage of cells) of different conditions each transfected at a different cell density from 2 to $5 \cdot 10^6$ cells/mL. **F)** Growth curve of HEK293 in batch culture using FreeStyle F17 medium. Blue and red dotted lines indicate 80% and 50% of cell viability respectively. Solid orange and blue lines represent glucose and lactate respectively monitored throughout the culture.

Figure 2. Analysis of relevant differences between 2hpt and 72hpt . **A)** Venn diagram of proteins identified with more than 1 peptide at 2 hpt (667 proteins), 72 hpt (401 proteins) and both (3335 proteins) all present in the three studied conditions. **B)** Biological processes significantly enriched related to the 667 unique proteins found at 2hpt. **C)** Biological processes significantly enriched related to the 401 unique proteins found at 72hpt. **D)** Western blot of p24 of Gag polyprotein. **E)** Venn diagram representing up and downregulated proteins and processes at 2 and 72hpt.

Figure 3. Protein changes related to cell growth. **A)** Representation of the proteins showing up or downregulations in the three studied conditions: N (no transfected), M (transfected with mock) and S (standard transfection) at the same time, from 2 to 72hpt. Different colours represent the different analysed groups of proteins. **B)** Western blots

of relevant proteins from each group of interest. I, II and III represent the biological replicates. **C)** Dot plots showing the change in expression from 2hpt to 72hpt from these relevant proteins. Variations are calculated using the 9 biological replicates. Medians are represented by horizontal bars. *p-values* are calculated using Mann Whitney U test.

Figure 4. Altered biological processes due to transfection. **A)** Processes upregulated upon transfection. **B)** Processes whose downregulation is prevented by transfection. **C)** Processes downregulated by transfection. **D)** Processes whose upregulation is prevented by transfection. Blue and green represent non-transfected and transfected condition respectively.

Figure 5. Heat map showing main changes upon VLP production. Colours represent Zq of each protein in each condition. Conditions are denoted by N (no transfected), M (transfected with mock) and S (standard transfection).

Figure 6. A) Heat map showing all components of the different ESCRT complexes at 2 and 72 hpt. Colours represent Zq of each protein in each condition. Conditions are denoted by N (no transfected), M (transfected with mock) and S (standard transfection). **B**) Box plots representations of the Zq values composing the different ESCRT complexes at 2 and 72hpt. Medians are represented by vertical bars and whiskers extend to extreme data points. *p-values* are calculated using Mann Whitney U test. *p-values* are calculated using Mann Whitney U test.

Figure 7. Summary of quantified changes present in all conditions (Cell density effect), present in transfected conditions (transfection effect) and present only in the VLP-producing condition (production effect).

REFERENCES

1. Bandaranayake, A. D. & Almo, S. C. Recent advances in mammalian protein production. *FEBS Lett* **588**, 253–260 (2014).
2. Roldão, A., Mellado, M. C., Castilho, L. R., Carrondo, M. J. & Alves, P. M. Virus-like particles in vaccine development. *Expert Rev Vaccines* **9**, 1149–1176 (2010).
3. Nascimento, I. & Leite, L. Recombinant vaccines and the development of new vaccine strategies. in *Braz J Med Biol Res* **45**, 1102–1111 (2012).
4. Gurramkonda, C. *et al.* Purification of hepatitis B surface antigen virus-like particles from recombinant Pichia pastoris and in vivo analysis of their immunogenic properties. *J Chromatogr B Anal. Technol Biomed Life Sci* **940**, 104–111 (2013).
5. Bell, N. M. & Lever, A. M. HIV Gag polyprotein: processing and early viral particle assembly. *Trends Microbiol* **21**, 136–144 (2013).
6. Meng, B. & Lever, A. M. Wrapping up the bad news: HIV assembly and release. *Retrovirology* **10**, 5 (2013).
7. von Schwedler, U. K. *et al.* The protein network of HIV budding. *Cell* **114**, 701–713 (2003).
8. Henne, W. M., Buchkovich, N. J. & Emr, S. D. The ESCRT pathway. *Dev Cell* **21**, 77–91 (2011).
9. Wollert, T. *et al.* The ESCRT machinery at a glance. in *J Cell Sci* **122**, 2163–2166 (2009).
10. Scourfield, E. J. & Martin-Serrano, J. Growing functions of the ESCRT machinery in cell biology and viral replication. *Biochem Soc Trans* **45**, 613–634 (2017).
11. Fujii, K., Hurley, J. H. & Freed, E. O. Beyond Tsg101: the role of Alix in 'ESCRTing' HIV-1. *Nat Rev Microbiol* **5**, 912–916 (2007).
12. McCullough, J., Fisher, R. D., Whitby, F. G., Sundquist, W. I. & Hill, C. P. ALIX-CHMP4 interactions in the human ESCRT pathway. *Proc Natl Acad Sci U S A* **105**, 7687–7691 (2008).
13. Alonso, Y. A. M., Migliano, S. M. & Teis, D. ESCRT-III and Vps4: a dynamic multipurpose tool for membrane budding and scission. *Febs j* **283**, 3288–3302 (2016).

14. Langelier, C. *et al.* Human ESCRT-II complex and its role in human immunodeficiency virus type 1 release. *J Virol* **80**, 9465–9480 (2006).

15. Meng, B., Ip, N. C., Prestwood, L. J., Abbink, T. E. & Lever, A. M. Evidence that the endosomal sorting complex required for transport-II (ESCRT-II) is required for efficient human immunodeficiency virus-1 (HIV-1) production. *Retrovirology* **12**, 72 (2015).

16. Chung, H. Y. *et al.* NEDD4L overexpression rescues the release and infectivity of human immunodeficiency virus type 1 constructs lacking PTAP and YPXL late domains. *J Virol* **82**, 4884–4897 (2008).

17. Usami, Y., Popov, S., Popova, E. & Gottlinger, H. G. Efficient and specific rescue of human immunodeficiency virus type 1 budding defects by a Nedd4-like ubiquitin ligase. *J Virol* **82**, 4898–4907 (2008).

18. Pincetic, A. & Leis, J. The Mechanism of Budding of Retroviruses From Cell Membranes. *Adv Virol* **2009**, 6239691–6239699 (2009).

19. Hurley, J. H. ESCRT complexes and the biogenesis of multivesicular bodies. *Curr Opin Cell Biol* **20**, 4–11 (2008).

20. Dyson, M. R. Fundamentals of Expression in Mammalian Cells. *Adv Exp Med Biol* **896**, 217–224 (2016).

21. Bussow, K. Stable mammalian producer cell lines for structural biology. *Curr Opin Struct Biol* **32**, 81–90 (2015).

22. Ausubel, L. J. *et al.* Production of CGMP-Grade Lentiviral Vectors. *Bioprocess Int* **10**, 32–43 (2012).

23. Merten, O. W. *et al.* Large-scale manufacture and characterization of a lentiviral vector produced for clinical ex vivo gene therapy application. *Hum Gene Ther* **22**, 343–356 (2011).

24. Geisse, S. & Fux, C. Recombinant protein production by transient gene transfer into Mammalian cells. *Methods Enzym.* **463**, 223–238 (2009).

25. Cervera, L. *et al.* Generation of HIV-1 Gag VLPs by transient transfection of HEK 293 suspension cell cultures using an optimized animal-derived component free medium. *J Biotechnol* **166**, 152–165 (2013).

26. Geisse, S. Reflections on more than 10 years of TGE approaches. *Protein Expr Purif* **64**, 99–107 (2009).

27. Tuvesson, O., Uhe, C., Rozkov, A. & Lullau, E. Development of a generic transient transfection process at 100 L scale. *Cytotechnology* **56**, 123–136 (2008).

28. Backliwal, G., Hildinger, M., Hasija, V. & Wurm, F. M. High-density transfection with HEK-293 cells allows doubling of transient titers and removes need for a priori DNA complex formation with PEI. *Biotechnol Bioeng* **99**, 721–727 (2008).

29. Huynh, H. T., Tran, T. T., Chan, L. C., Nielsen, L. K. & Reid, S. Effect of the peak cell density of recombinant AcMNPV-infected Hi5 cells on baculovirus yields. *Appl Microbiol Biotechnol* **99**, 1687–1700 (2015).

30. Genzel, Y. *et al.* High cell density cultivations by alternating tangential flow (ATF) perfusion for influenza A virus production using suspension cells. *Vaccine* **32**, 2770–2781 (2014).

31. Clincke, M. F. *et al.* Very high density of CHO cells in perfusion by ATF or TFF in WAVE bioreactor. Part I. Effect of the cell density on the process. *Biotechnol Prog* **29**, 754–767 (2013).

32. Gutiérrez-Granados, S., Cervera, L., Gòdia, F., Carrillo, J. & Segura, M. M. Development and validation of a quantitation assay for fluorescently tagged HIV-1 virus-like particles. *J Virol Methods* **193**, 85–95 (2013).

33. Cheeks, M. C., Edwards, A. D., Arnot, C. J. & Slater, N. K. H. Gene transfection of HEK cells on supermacroporous polyacrylamide monoliths: A comparison of transient and stable recombinant protein expression in perfusion culture. *N. Biotechnol.* **26**, 289–299 (2009).

34. Wiśniewski, J. R., Zougman, A., Nagaraj, N. & Mann, M. Universal sample preparation method for proteome analysis. *Nat. Methods* **6**, 359–362 (2009).

35. Martínez-Bartolomé, S. *et al.* Properties of average score distributions of SEQUEST: the probability ratio method. *Mol. Cell. Proteomics* **7**, 1135–45 (2008).

36. Bonzon-Kulichenko, E., Garcia-Marques, F., Trevisan-Herraz, M. & Vazquez, J. Revisiting peptide identification by high-accuracy mass spectrometry: problems associated with the use of narrow mass precursor windows. *J Proteome Res* **14**, 700–710 (2015).

37. Navarro, P. *et al.* General statistical framework for quantitative proteomics by stable isotope labeling. *J Proteome Res* **13**, 1234–1247 (2014).

38. Martínez-Acedo, P. *et al.* A novel strategy for global analysis of the dynamic thiol redox proteome. *Mol. Cell. Proteomics* **11**, 800–13 (2012).

39. Trevisan-Herraz, M. *et al.* SanXoT: a modular and versatile package for the quantitative analysis of high-throughput proteomics experiments. *Bioinformatics* **35**, 1594–1596 (2019).

40. Garcia-Marques, F. *et al.* A Novel Systems-Biology Algorithm for the Analysis of Coordinated Protein Responses Using Quantitative Proteomics. *Mol Cell Proteomics* **15**, 1740–1760 (2016).

41. Navarro, P. *et al.* General statistical framework for quantitative proteomics by stable isotope labeling. *J. Proteome Res.* **13**, 1234–47 (2014).

42. García-Marqués, F. *et al.* A Novel Systems-Biology Algorithm for the Analysis of Coordinated Protein Responses Using Quantitative Proteomics. *Mol. Cell. Proteomics* **15**, 1740–60 (2016).

43. Ashburner, M. *et al.* Gene Ontology: tool for the unification of biology. *Nat. Genet.* **25**, 25–29 (2000).

44. The Gene Ontology Consortium. Expansion of the Gene Ontology knowledgebase and resources. *Nucleic Acids Res.* **45**, D331–D338 (2017).

45. Huang da, W., Sherman, B. T. & Lempicki, R. A. Systematic and integrative analysis of large gene lists using DAVID bioinformatics resources. *Nat Protoc* **4**, 44–57 (2009).

46. Huang da, W., Sherman, B. T. & Lempicki, R. A. Bioinformatics enrichment tools: paths toward the comprehensive functional analysis of large gene lists. *Nucleic Acids Res* **37**, 1–13 (2009).

47. Fabregat, A. *et al.* The Reactome Pathway Knowledgebase. *Nucleic Acids Res.* **46**, D649–D655 (2018).

48. Schneider, C. A., Rasband, W. S. & Eliceiri, K. W. NIH Image to ImageJ: 25 years of image analysis. *Nat. Methods* **9**, 671–5 (2012).

49. Cervera, L., Gonzalez-Dominguez, I., Segura, M. M. & Godia, F. Intracellular characterization of Gag VLP production by transient transfection of HEK 293 cells. *Biotechnol Bioeng* **114**, 2507–2517 (2017).

50. Ding, J., Zhao, J., Sun, L., Mi, Z. & Cen, S. Citron kinase enhances ubiquitination of HIV-1 Gag protein and intracellular HIV-1 budding. *Arch Virol* **161**, 2441–2448 (2016).

51. Ferreira, T. B., Carrondo, M. J. & Alves, P. M. Effect of ammonia production on intracellular pH: Consequent effect on adenovirus vector production. *J Biotechnol* **129**, 433–438 (2007).

52. Le Ru, A. *et al.* Scalable production of influenza virus in HEK-293 cells for efficient vaccine manufacturing. *Vaccine* **28**, 3661–3671 (2010).

53. Petiot, E., Cuperlovic-Culf, M., Shen, C. F. & Kamen, A. Influence of HEK293 metabolism on the production of viral vectors and vaccine. *Vaccine* **33**, 5974–5981 (2015).

54. Yang, S., Zhou, X., Li, R., Fu, X. & Sun, P. Optimized PEI-based Transfection Method for Transient Transfection and Lentiviral Production. *Curr Protoc Chem Biol* **9**, 147–157 (2017).

55. Robert, M. A. *et al.* Manufacturing of recombinant adeno-associated viruses using mammalian expression platforms. *Biotechnol J* **12**, (2017).

56. Bernal, V., Carinhas, N., Yokomizo, A. Y., Carrondo, M. J. & Alves, P. M. Cell density effect in the baculovirus-insect cells system: a quantitative analysis of energetic metabolism. *Biotechnol Bioeng* **104**, 162–180 (2009).

57. Rajendra, Y., Balasubramanian, S. & Hacker, D. L. Large-Scale Transient Transfection of Chinese Hamster Ovary Cells in Suspension. *Methods Mol Biol* **1603**, 45–55 (2017).

58. Bereiter-Hahn, J., Munnich, A. & Woiteneck, P. Dependence of energy metabolism on the

density of cells in culture. *Cell Struct Funct* **23**, 85–93 (1998).

59. Henry, O., Perrier, M. & Kamen, A. Metabolic flux analysis of HEK-293 cells in perfusion cultures for the production of adenoviral vectors. *Metab Eng* **7**, 467–476 (2005).

60. Fuenmayor, J., Cervera, L., Gòdia, F. & Kamen, A. Extended gene expression for Gag VLP production achieved at bioreactor scale. *J. Chem. Technol. Biotechnol.* **94**, 302–308 (2019).

61. Bai, H., Lester, G. M. S., Petishnok, L. C. & Dean, D. A. Cytoplasmic transport and nuclear import of plasmid DNA. *Biosci Rep* **37**, (2017).

62. Chahal, P. S., Schulze, E., Tran, R., Montes, J. & Kamen, A. A. Production of adeno-associated virus (AAV) serotypes by transient transfection of HEK293 cell suspension cultures for gene delivery. *J Virol Methods* **196**, 163–173 (2014).

63. Fuenmayor, J., Cervera, L., Gutierrez-Granados, S. & Godia, F. Transient gene expression optimization and expression vector comparison to improve HIV-1 VLP production in HEK293 cell lines. *Appl Microbiol Biotechnol* **102**, 165–174 (2018).

64. Hall, A., Lachelt, U., Bartek, J., Wagner, E. & Moghimi, S. M. Polyplex Evolution: Understanding Biology, Optimizing Performance. *Mol Ther* **25**, 1476–1490 (2017).

65. Vukelic, Z. & Kalanj-Bognar, S. Cell density-dependent changes of glycosphingolipid biosynthesis in cultured human skin fibroblasts. *Glycoconj J* **18**, 429–437 (2001).

66. Sillence, D. J. *et al.* Glucosylceramide modulates membrane traffic along the endocytic pathway. *J Lipid Res* **43**, 1837–1845 (2002).

67. Kamau, S. W., Kramer, S. D., Gunthert, M. & Wunderli-Allenspach, H. Effect of the modulation of the membrane lipid composition on the localization and function of P-glycoprotein in MDR1-MDCK cells. *Vitr. Cell Dev Biol Anim* **41**, 207–216 (2005).

68. Lippincott-Schwartz, J. & Phair, R. D. Lipids and cholesterol as regulators of traffic in the endomembrane system. *Annu Rev Biophys* **39**, 559–578 (2010).

69. Lingwood, C. A. Glycosphingolipid functions. *Cold Spring Harb Perspect Biol* **3**, (2011).

70. Gorlach, A., Bertram, K., Hudecova, S. & Krizanova, O. Calcium and ROS: A mutual interplay. *Redox Biol* **6**, 260–271 (2015).

71. Takahashi, A. *et al.* Exosomes maintain cellular homeostasis by excreting harmful DNA from cells. *Nat Commun* **8**, 15287 (2017).

72. Loomis, R. J. *et al.* Citron Kinase, a RhoA Effector, Enhances HIV-1 Virion Production by Modulating Exocytosis. *Traffic* **7**, 1643–1653 (2006).

73. Perlman, M. & Resh, M. D. Identification of an intracellular trafficking and assembly pathway for HIV-1 gag. *Traffic* **7**, 731–45 (2006).

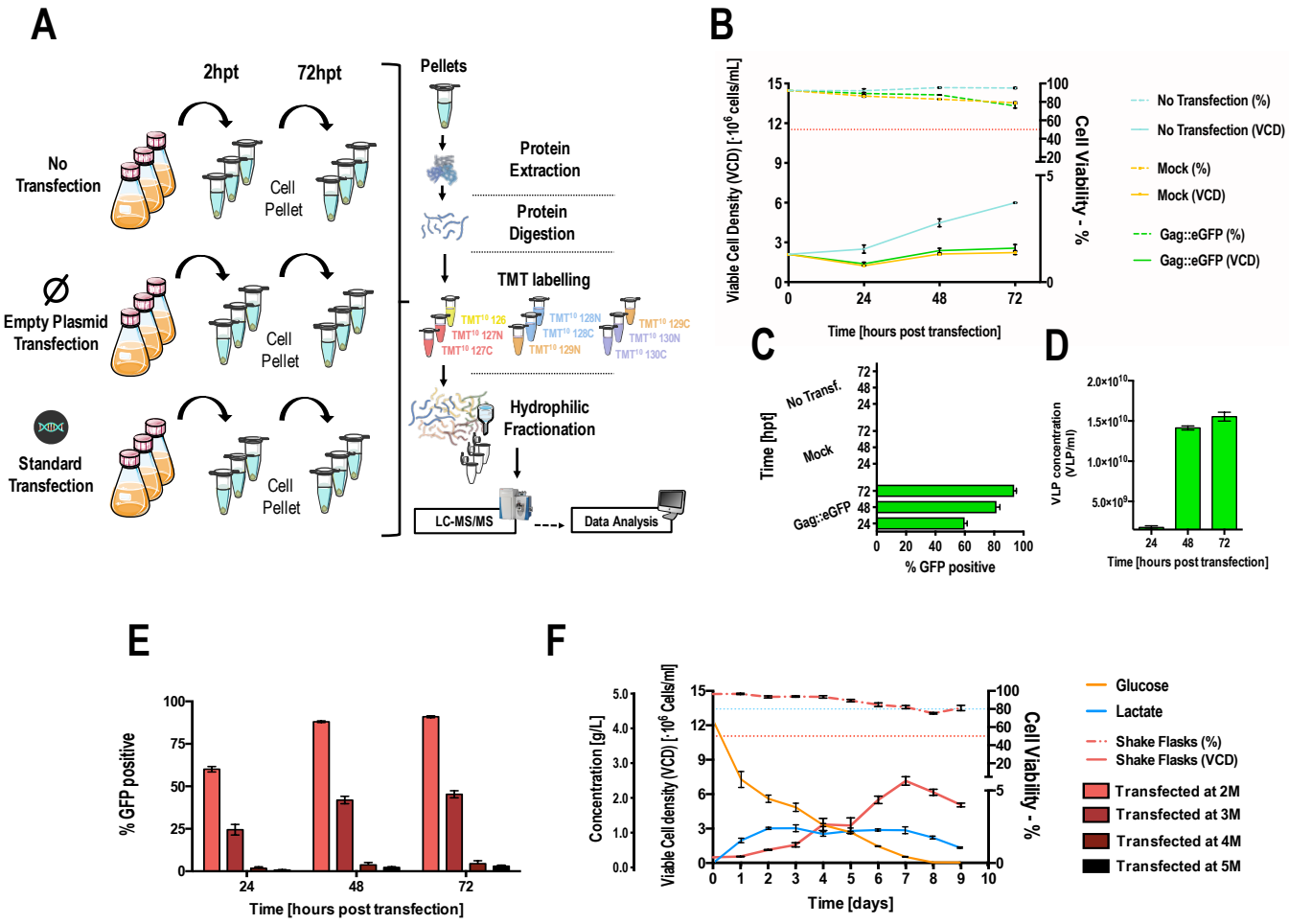

Figure 1. Experimental design and cell growth and VLP production data. **A)** Experimental workflow. Three biological replicates of HEK293 cells were cultured in three different conditions. No transfected condition, transfected with an empty plasmid denoted as 'mock' and transfected using the standard protocol with the plasmid containing the gene gag::egfp gene. Both transfections were performed at the same cell density of $2 \cdot 10^6$ cells/mL. At the time point of 2 hours post transfection (hpt) cultured samples were taken, centrifuged and cellular pellets were stored at -80ºC. Same procedure was repeated at 72hpt. Proteins were extracted from the pellet samples, digested and peptides were labelled using Tandem Mass Tag (TMT) labelling. Labelled peptides were fractionated and analysed via LC-MS/MS. **B)** Viable cell density and cell viability graphs along the time course. The red dotted line indicates 50% of cell viability. Cells were transfected at time point 0. **C)** Flow cytometry analysis of the transfection percentage (showed in GFP positive percentage of cells) in the different conditions along the time course. **D)** VLP concentration in the supernatants of the standard transfection condition along the time course, showing the production of VLPs. **E)** Flow cytometry analysis of the transfection percentage (showed in GFP positive percentage of cells) of different conditions each transfected at a different cell density from 2 to $5 \cdot 10^6$ cells/mL. **F)** Growth curve of HEK293 in batch culture using FreeStyle F17 medium. Blue and red dotted lines indicate 80% and 50% of cell viability respectively. Solid orange and blue lines represent glucose and lactate respectively monitored throughout the culture.

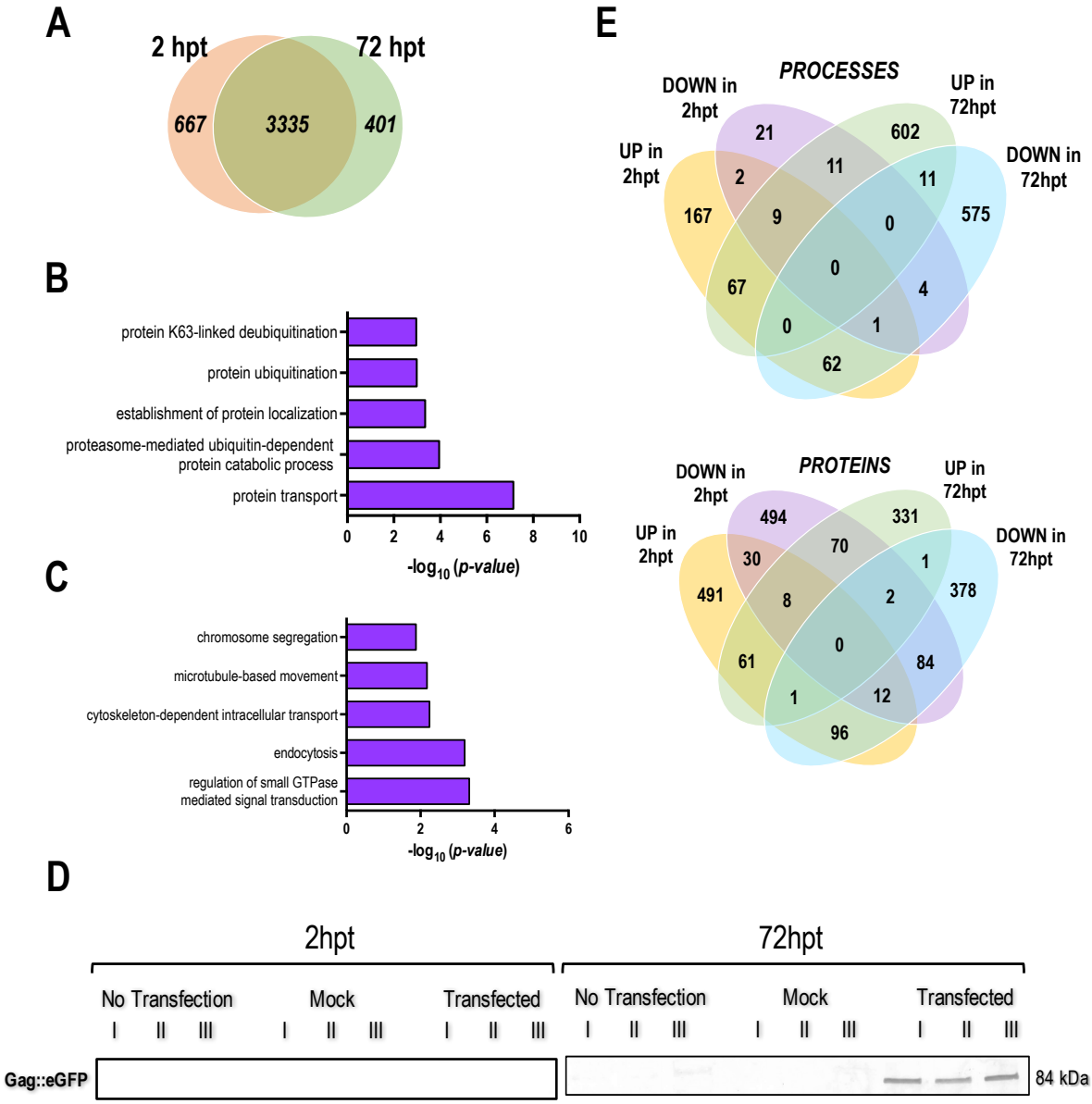

Figure 2. Analysis of relevant differences between 2hpt and 72hpt . **A)** Venn diagram of proteins identified with more than 1 peptide at 2 hpt (667 proteins), 72 hpt (401 proteins) and both (3335 proteins) all present in the three studied conditions. **B)** Biological processes significantly enriched related to the 667 unique proteins found at 2hpt. **C)** Biological processes significantly enriched related to the 401 unique proteins found at 72hpt. **D)** Western blot of p24 of Gag polyprotein. **E)** Venn diagram representing up and downregulated proteins and processes at 2 and 72hpt.

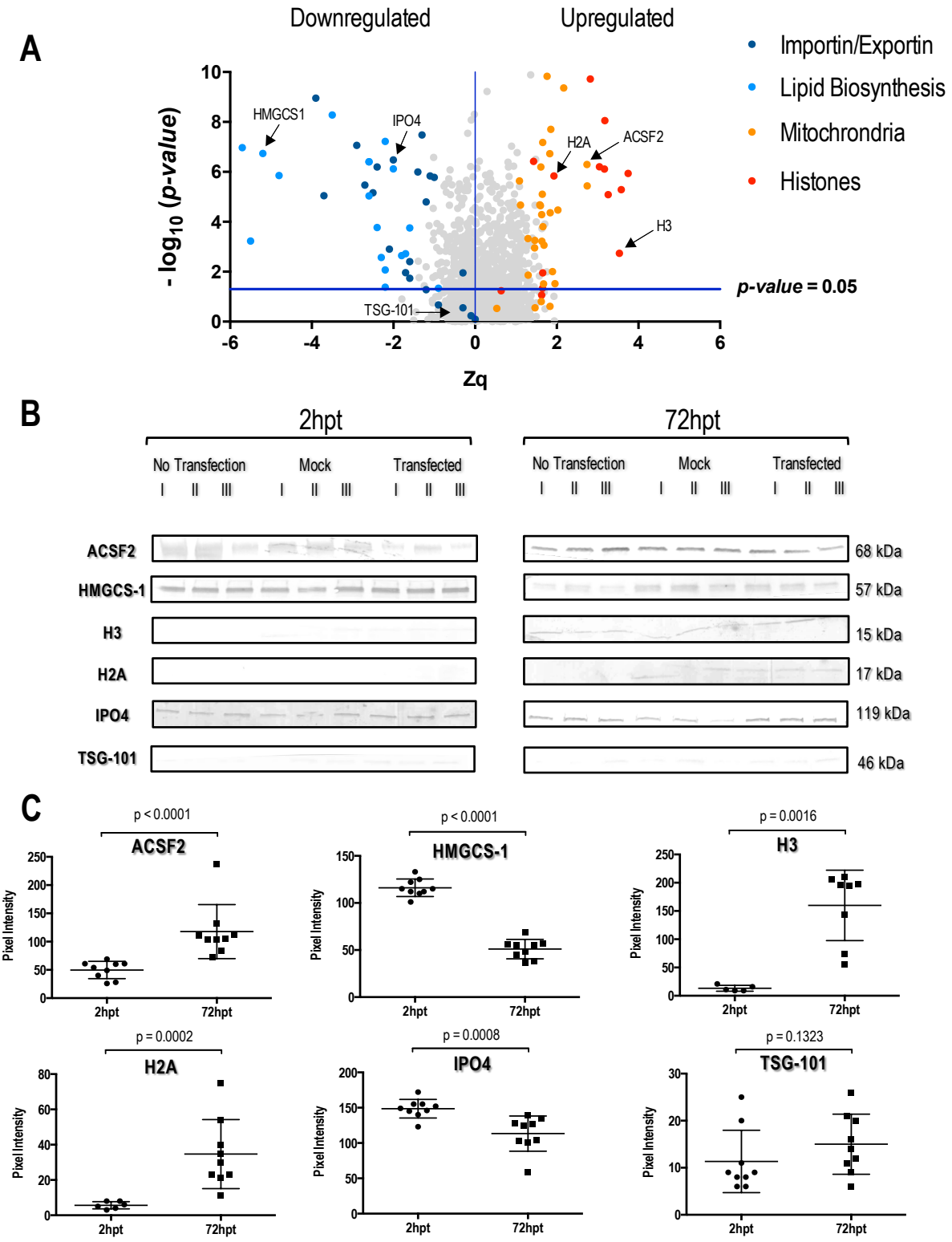

Figure 3. Protein changes related to cell growth. **A)** Representation of the proteins showing up or downregulations in the three studied conditions: N (no transfected), M (transfected with mock) and S (standard transfection) at the same time, from 2 to 72hpt. Different colours represent the different analysed groups of proteins. **B)** Western blots of relevant proteins from each group of interest. I, II and III represent the biological replicates. **C)** Dot plots showing the change in expression from 2hpt to 72hpt from these relevant proteins. Variations are calculated using the 9 biological replicates. Medians are represented by horizontal bars. *p-values* are calculated using Mann Whitney U test.

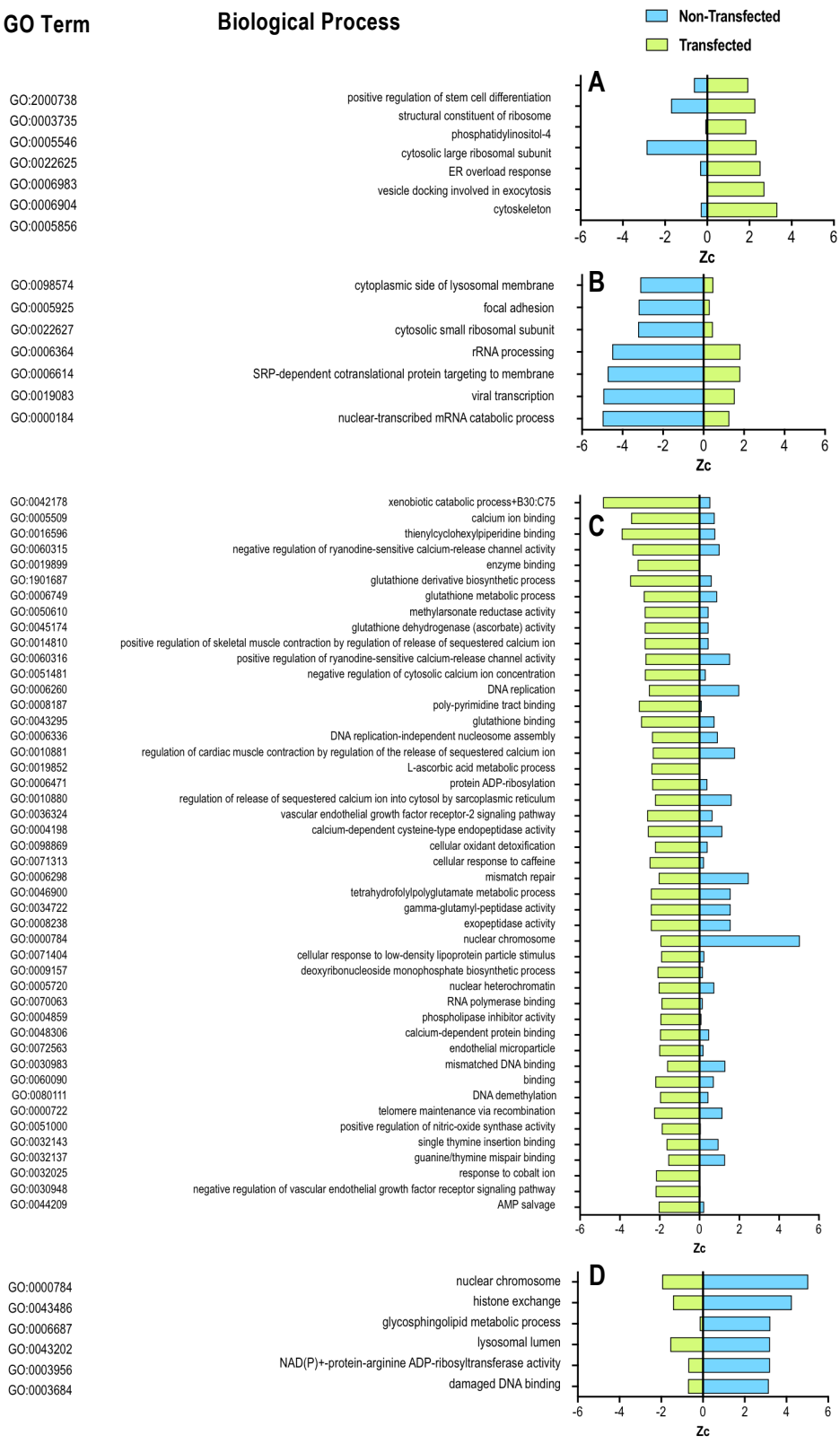

Figure 4. Altered biological processes due to transfection. **A)** Processes upregulated upon transfection. **B)** Processes whose downregulation is prevented by transfection. **C)** Processes downregulated by transfection. **D)** Processes whose upregulation is prevented by transfection. Blue and green represent non-transfected and transfected condition respectively.

Figure 5. Heat map showing main changes upon VLP production. Colours represent Zq of each protein in each condition. Conditions are denoted by N (no transfected), M (transfected with mock) and S (standard transfection).

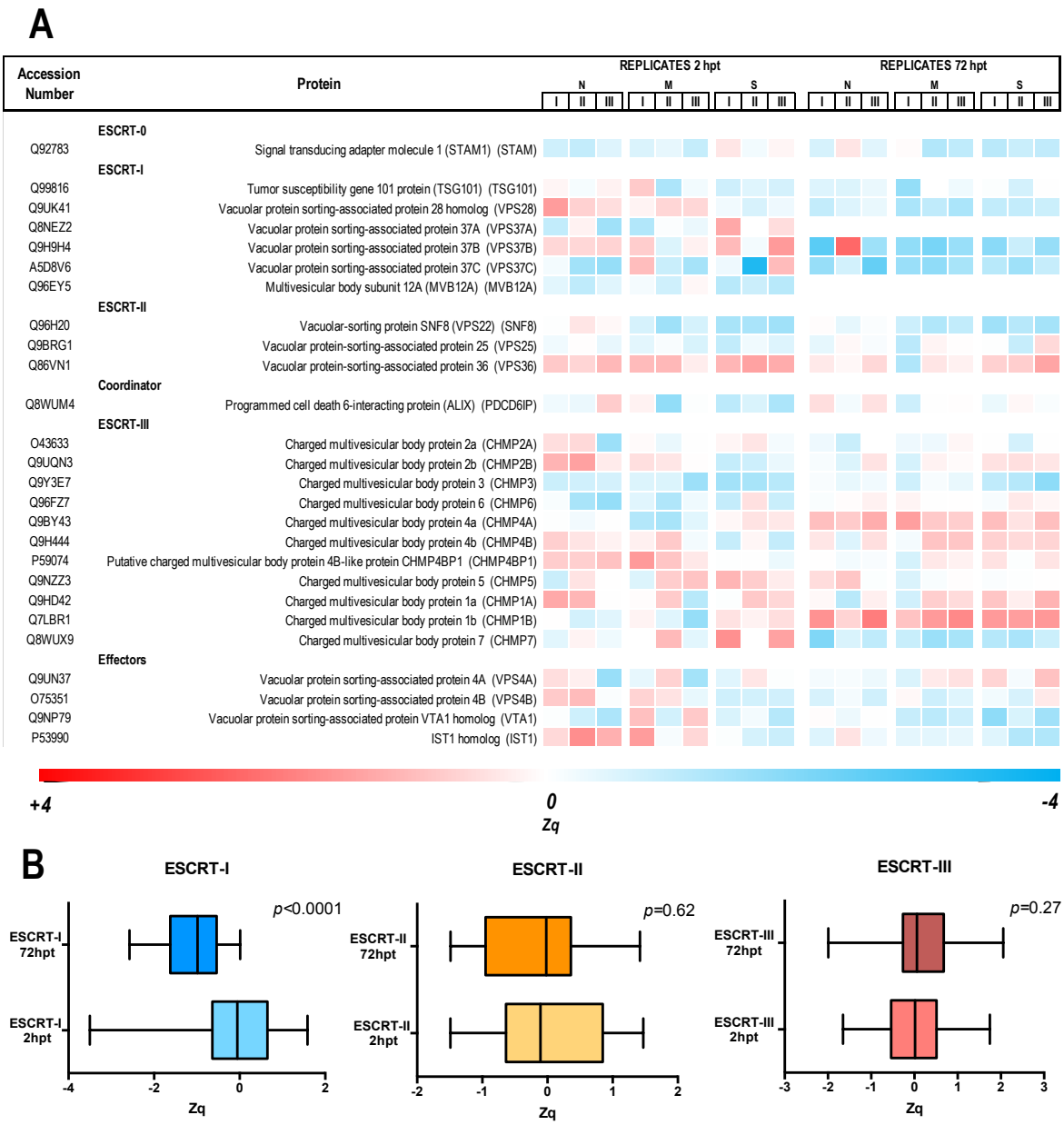

Figure 6. A) Heat map showing all components of the different ESCRT complexes at 2 and 72 hpt. Colours represent Zq of each protein in each condition. Conditions are denoted by N (no transfected), M (transfected with mock) and S (standard transfection). **B**) Box plots representations of the Zq values composing the different ESCRT complexes at 2 and 72hpt. Medians are represented by vertical bars and whiskers extend to extreme data points. *p-values* are calculated using Mann Whitney U test. *p-values* are calculated using Mann Whitney U test.

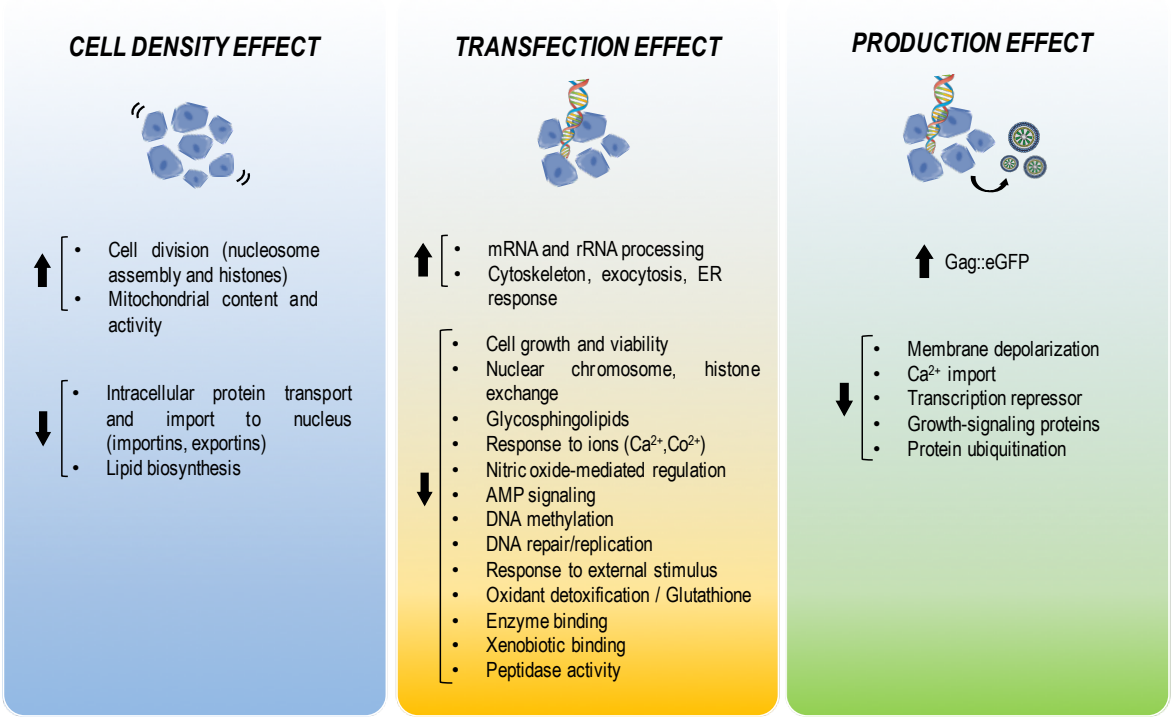

Figure 7. Summary of quantified changes present in all conditions (Cell density effect), present in transfected conditions (transfection effect) and present only in the VLP-producing condition (production effect).

Supporting Information

Multiplexed quantitative proteomic analysis of HEK293 provides insights of molecular changes associated to the cell density effect, transient transfection and virus-like particles production.

Authors: Jesús Lavado-García*[1], Inmaculada Jorge[2-3], Laura Cervera[1], Jesús Vázquez[2-3], Francesc Gòdia[1]

[1]Grup d'Enginyeria Cellular i Bioprocés, Departament d'Enginyeria Química, Biològica i Ambiental, Escola d'Enginyeria, Universitat Autònoma de Barcelona, Campus de Bellaterra, Cerdanyola del Vallès, 08193 Barcelona, Spain

[2]Laboratory of Cardiovascular Proteomics, Centro Nacional Investigaciones Cardiovasculares (CNIC), C/ Melchor Fernández Almagro 3, Madrid 28029, Spain

[3]Centro de Investigación Biomédica en Red Enfermedades Cardiovasculares (CIBERCV), Madrid, Spain

*Corresponding Author:

Jesús Lavado-García (e-mail: jesus.lavado@uab.cat)

Table of Contents

Supplementary Figure S1. Decrease in transfection efficiency at high cell density in HyCell™ TransFx-H media. Flow cytometry analysis of the transfection percentage (showed in GFP positive percentage of cells) and RFU measurement of different conditions each transfected at a different cell density from 2 to $5 \cdot 10^6$ cells/mL in HyCell™ TransFx-H (HyClone) media.

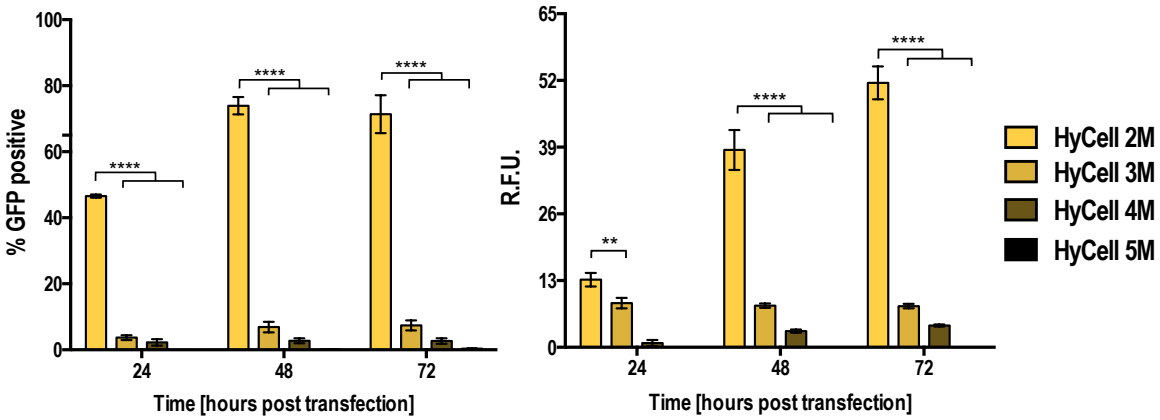

Supplementary Table S1. List of all Identified proteins in this study. Biological replicates are denotated by (I,II,III). Significant FDR shown in bold. Gag::eGFP protein highlighted in yellow. Color scale show upregulation (red) and downregulation (blue).

(Excel file)